Journal of Electron Spectroscopy and Related Phenomena 281 (2025) 147544

Contents lists available at ScienceDirect

Journal of Electron Spectroscopy and Related Phenomena

journal homepage: www.elsevier.com/locate/elspec

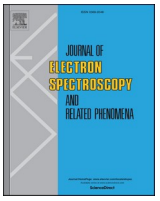

Recoil effects in high energy photoemission of solids – Revisited

F. Roth [a,b], D. Potorochin [a,b,c], A. Gloskovskii [c], C. Schlueter [c], L. Wenthaus [c], S. Molodtsov [a,b,d], W. Drube [c], W. Eberhardt [c,*]

[a] Institute of Experimental Physics, TU Bergakademie Freiberg, Freiberg D-9599, Germany
[b] Center for Efficient High Temperature Processes and Materials Conversion (ZeHS), TU Bergakademie Freiberg, Freiberg 09599, Germany
[c] Deutsches Elektronen-Synchrotron DESY, Notkestrasse 85, Hamburg D-22607, Germany
[d] European XFEL GmbH, Holzkoppel 4, 22869, Schenefeld D-22869, Germany

ARTICLE INFO

Keywords:
HAXPES
Core-level recoil effects
Silicon carbide
Synchrotron radiation

ABSTRACT

This study systematically investigates core level recoil in photoemission from crystalline silicon (Si) and silicon carbide (4H-SiC), within the X-ray range of 2.45–9.5 keV. By examining the Si 2p, 2s, and C 1s core levels, we observe that SiC exhibits energy shifts exceeding single-atom recoil predictions, along with a lineshape change at higher photon energies attributed to being phonon-induced. In contrast, pure Si shows more modest shifts and line broadening, consistent with expected recoil effects. These observations imply that especially compound materials, such as SiC, exhibit an enhanced interplay of recoil and phonon dynamics, underscoring the necessity for refined photoemission models that accommodate these effects.

1. Introduction

The physics of recoil in photoemission appears straightforward and readily described when considering gas phase XPS of small and even larger molecules is concerned. The momentum of the photoemitted electron is balanced by the center-of-mass momentum of the molecule. Beyond this conservation of total momentum, vibrational and rotational excitations accompany the photoemission process [1]. Even the Doppler broadening due to the thermal motion of the molecule in the gas phase can be incorporated into the description of the photoemission process and the resulting lineshape [2].

In solids, phonon sidebands are generally not resolved in photoemission, instead manifesting themselves as a change in lineshape. The momentum conservation is observable as an apparent shift of the photoemission lines to higher binding energies upon increasing the excitation energy. Recent advances in high-resolution beamlines in the so-called tender X-ray range (from 2 keV to 10 keV photon energy) at various synchrotron facilities have enabled these studies. Using a crystal monochromator in near back reflection geometry allows for resolutions in the 10 meV range at certain photon energies up to and beyond 10 keV. The first beamline of this kind available for user operation was installed at SPRING 8 [3] and accordingly, most of the initial work was performed there. An overview of the numerous beamlines now available for this type of research is provided in [4].

Recent years have seen a number of studies on the recoil process in solids, but the results have shown some inconsistencies. The first observation of the effect dates back to 2007 by Takata et al. [5], where the C 1s photoemission of graphite was measured across a large range of excitation energies from 340 eV to 7940 eV. The first surprise in the data was that the C 1s spectrum taken at 870 eV photon energy exhibited a shift of about 100 meV to lower binding energy when compared to the spectrum taken at 340 eV photon energy. This is just the opposite of what is expected for the recoil effect. Takata et al. [5] attributed this shift to surface core level emission, which is prominent at 340 eV and presumed to be almost absent at 870 eV. However, this explanation is not convincing, given that the escape depth changes by less than a factor of 2 - from about 5 Å to 8 Å – over this range of excitation energies.

The unbiased observer was even more surprised when recoil effects were observed at the Fermi edge in metals such as Al as compared to Au. After excitation at a photon energy of 7940 eV, the Al Fermi edge shifted by 120 meV and broadened substantially [6]. This shift is only slightly less than 138 meV predicted by a simple single-atom recoil estimate for Al [6]. This observation is counterintuitive, given that valence electrons in simple metals are generally considered to be delocalized throughout the entire solid. Even though the regions of the wavefunctions close to the nuclei predominantly contribute to the photoemission intensity [7], it is multiple nuclei — not just a single one—that contribute to the photoemission intensity of the valence band.

* Corresponding author.
E-mail address: wolfgang.eberhardt@cfel.de (W. Eberhardt).

https://doi.org/10.1016/j.elspec.2025.147544
Received 16 February 2025; Received in revised form 20 May 2025; Accepted 27 May 2025
Available online 4 June 2025

The confusion deepens when examining the available data on (deep) core levels in compound materials. A recent study of lanthanum hexaboride (LaB_6) observed an agreement between the experimental recoil shifts and the calculated values. In this case, only the B 1 s showed a recoil shift, and none of the La core levels exhibited any detectable shift. This phenomenon can be explained by the high atomic weight of La in comparison to B [8]. In V_3Si the Si 2p level exhibits a recoil shift close to the expected value, but the V 2p level does not show this effect [9]. Other Vanadium containing compounds either do or don't show a recoil shift. This inconsistency is addressed in the paper entitled 'Do all nuclei recoil on photoemission in compounds?' by S. Suga et al. [10]. The authors explicitly state: 'The criterion for the presence or absence of recoil effects in solid compounds, including nucleus dependence, is a rather complicated problem', without providing further detailed elaboration. In view of this uncertainty, we refrain from citing or commenting on the interpretation of recoil shifts in the valence band region, apart from the above-mentioned Fermi level shift.

In this study, we aim to provide further insight into the phenomenon of core level recoil in solids by presenting data on crystalline Si and 4H-SiC, specifically for the Si 2p, 2s, and C 1s core levels. It is important to note that, in contrast to the majority of previous studies, all data were obtained at room temperature in this study. This distinction is significant, as elevated temperatures may enhance phonon-related contributions to the recoil effects. Before discussing the data, we focus on the calibration of the electron spectrometers. Reliably measuring small core level energy shifts at high kinetic energies in an HAXPES experiment is challenging. Establishing a binding energy shift of 100 meV or less at kinetic energies up to 8 keV or higher demands extreme precision, and we cannot rely solely on the energy calibration of the (typically commercial) electron spectrometer to maintain this accuracy across the full kinetic energy range of 2.45–9.5 keV used in this experiment. Additionally, the energy calibration of the X-ray monochromator across the corresponding photon energy range is also not guaranteed at this level of precision. Consequently, we take reference spectra at each data point across the energy range using the 4f and 3d core levels of Au as energy references for both, the photon beam as well as the electron spectrometer. Given the high mass of Au, recoil shifts are assumed to be negligible, with a maximum shift of 27 meV for the 4f level at 10 keV in the single-atom limit. Further details are provided in the next section.

We note that our colleagues in this field are well aware of these calibration challenges, and it is not intended to imply that their spectrometers are inaccurately calibrated. We mention it here to emphasize that these commercial spectrometers require special attention to calibration whenever new operational ranges are explored, a caveat we find applies universally to all instruments on the market.

2. Experimental

The experiments were conducted at the P22 beamline at DESY [11]. The Si 2p, 2s lines from single-crystal n-type Si(100) wafers and the Si 2p, Si 2s, and C 1s lines from 4H-SiC(0001) were recorded at five different photon energies ranging from 2.45 keV to 9.5 keV, using a Phoibos 225HV electron analyzer (Specs GmbH). The measurements were performed at room temperature in constant analyzer energy mode with a pass energy of 20 eV. The pressure in the analytical chamber remained in the 10^{-10} mbar range. For energy calibration, both samples were coated with a thin Au layer (a few nanometers) before being introduced into the UHV system. As previously mentioned, the Au 4 f photoemission lines served as references for both photon energy and analyzer kinetic energy scales. To account for any minimal drifts in photon or spectrometer energies during the experiment, measurements of the Si 2p, 2s, and C 1s spectra for the respective photon energies were carried out at short time intervals, alternating with the Au reference spectra. This approach ensured that any potential shifts could be detected and corrected throughout the measurement process.

XPS spectra fitting was performed using a Python script that utilized the Lmfit package [12] for curve fitting and the Matplotlib package [13] for data visualization. The experimental core-level spectra were fitted using a symmetric Gaussian-Lorentzian profile (Voigt model) with four fitting parameters: amplitude, center position, sigma (Gaussian contribution, where FWHM $= 2 * \sqrt{2 * \ln(2)} * \sigma$), and gamma (Lorentzian contribution, where FWHM $= 2 * \gamma$). To account for the contribution of inelastically scattered electrons, a Shirley-type background profile was applied [14]. The Au $4f_{7/2}$ reference binding energy was fixed at 84 eV for all XPS spectra [15]. A correction of the core level shifts by including the theoretical recoil shift of the Au 4f core level with a maximum value of 19.5 meV when comparing spectra measured at 9500 eV and 2450 eV was tested, but did not significantly change the results presented in the next section.

3. Results and discussion

We begin by presenting our results for crystalline Si. Fig. 1 shows spectra obtained at photon energies ranging from 2.45 keV to 9.5 keV for the Si 2p and Si 2s core levels, along with the Au 4f reference. The center of the photoemission peaks for the Si 2p and Si 2s lines shifts towards larger binding energies with increasing photon energy, which is consistent with the expected recoil shift. The blue line, marking the center of the lines at 2.45 keV, serves as a guide to illustrate this effect. In addition, the Si 2p lines exhibit broadening at the highest photon energies, which are largely attributed to changes in overall energy resolution, since the lines at 4600 eV are narrowest and this coincides with the best overall photon energy resolution (see Table 1). A minor surface oxide contribution is visible in the Si 2 s spectra, appearing around 3.65 eV higher in binding energy (green component), particularly at lower excitation energies. In the Si 2p spectra, this contribution would be located outside the displayed range.

The corresponding core level spectra of 4H-SiC are shown in Fig. 2. Notably, the spin-orbit splitting in the Si 2p lines is no longer resolved, as also observed in previous XPS studies [16]. This is attributed not only to phonon-induced broadening but also to differences in surface preparation. In contrast to hydrogen-terminated surfaces that were utilised in earlier studies, our samples were coated with multiple monolayers of Au to ensure precise energy calibration. This procedure potentially obscures more subtle spectral characteristics, such as spin-orbit splitting. Unlike pure Si, the SiC lattice supports infrared active, high energy optical phonons that are excited during the photoemission process, leading to a substantially larger unresolved phonon broadening of the XPS lines. The energy of the optical phonons of SiC is typically twice as high as in Si. Similar to the spectra for pure Si, low-intensity shoulder features appear at the higher binding energy side of the main peak in the SiC spectra, well separated in energy from the main lines. These features are attributed to Si atoms bound to oxygen as well as C atoms bound to carbon, as indicated by the green component in the fitted spectra. This has also been reported in other work [16].

Visual inspection of the raw data reveals that the centroid of the lines shifts to higher binding energies with increasing photon energy. These shifts are significantly larger than the expected values based on a single-atom recoil estimate, which is around 137 meV for Si and 320 meV for C. This corresponds to the recoil from a single atom where the core electron was initially located, as determined by the equation:

$$\Delta E = E_{kin}(m/M) = 545meV \bullet \quad E_{kin}(keV)/M. \tag{1}$$

Unexpectedly, the magnitude of this shift is larger than what the free-atom model predicts for both types of atoms in SiC. Between the two extreme excitation energies, the fitted value of the photoemission peak shifts by 395 meV for the Si 2p, 362 meV for the Si 2s, and 603 meV for the C 1s level. These values are given relative to the binding energy observed at the lowest excitation energy of 2.45 keV rather than in absolute terms.

A comparison of these results with existing data reveals that this is

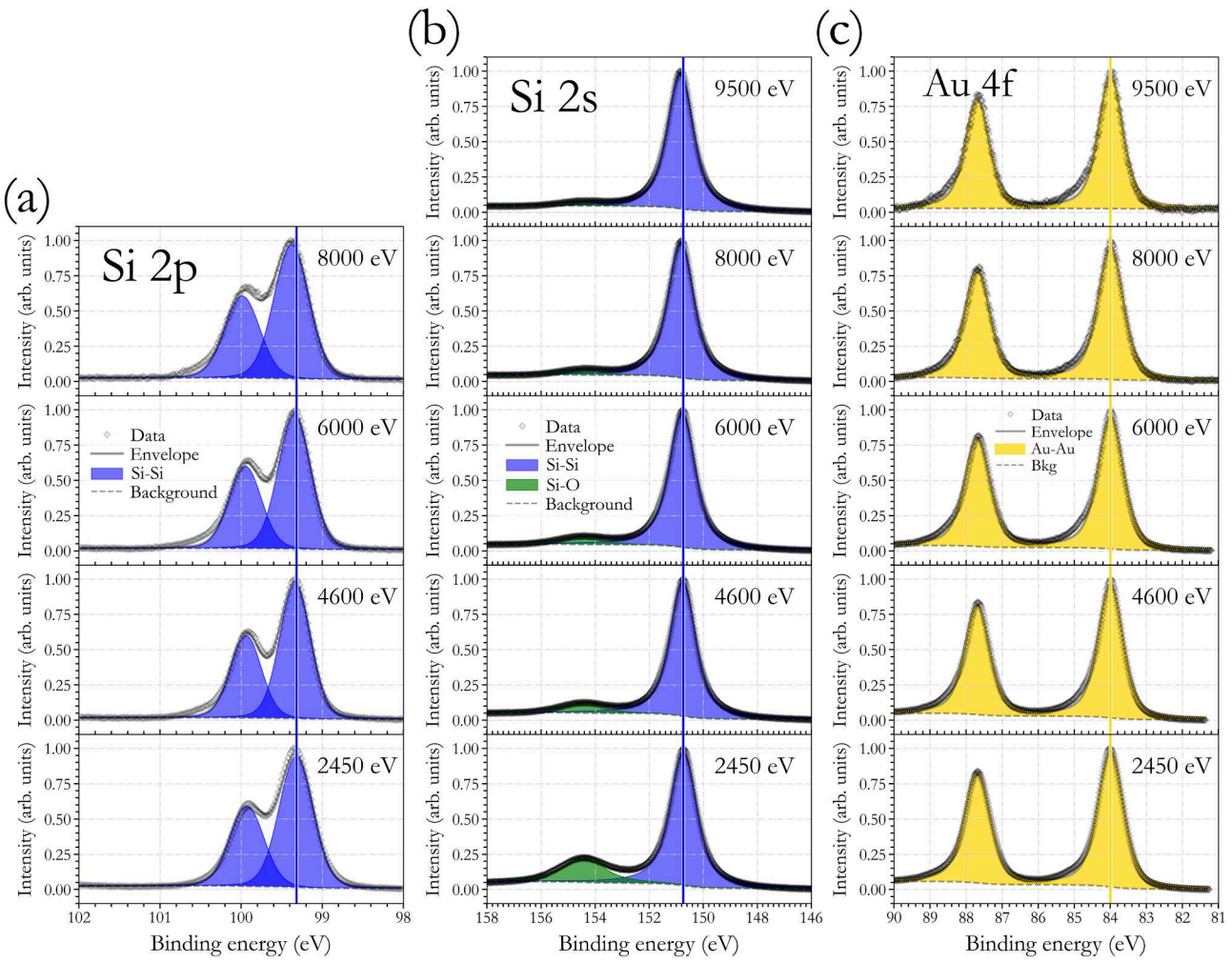

Fig. 1. HAXPES spectra of (a) the Si 2p, (b) Si 2s, and (c) Au 4f core levels of n-type Si(100) measured at 5 different photon energies ranging from 2.45 keV up to 9.5 keV at room temperature. The blue lines mark the centroid of the $2p_{3/2}$ and 2s core levels respectively at a photon energy of 2.45 keV. The Au 4f spectra serve as reference points for binding energy calibration.

Table 1
Energy resolution (FWHM) of the beamline at the photon energies used in this experiment. A double-crystal monochromator was employed, using Si(111) crystals at 2.45 keV and Si(311) crystals at higher energies. Resolutions were calculated using dynamical diffraction theory, accounting for the photon source characteristics and beamline configuration. The effective vertical angular acceptance was 20 μrad.

Photon Energy (eV)	2450	4600	6000	8000	9500
Resolution (meV)	217	121	197	342	480

the only instance where the observed centroid shift of the overall lineshape exceeds the predictions of the single-atom recoil model. In all other cases reported so far, measured shifts were either smaller than or barely reached the single-atom limit. For comparison, we refer to the results for crystalline Si shown in Fig. 1, where shifts are markedly smaller than those for SiC, as shown in Fig. 2. In crystalline Si, shifts range only around 80–100 meV, with detailed evaluations obtained using a fitting procedure that accounts for changes in lineshape. It is important to note that the discrepancy between the two Si core levels can be viewed as a limitation on the accuracy of the recoil shift determination. This is due to the assumption that in pristine silicon, both core levels should exhibit a similar shift.

This brings us to an analysis of the observed lineshapes. We begin with the data for crystalline Si, shown in Fig. 1. The deconvolution included in Fig. 1 clearly shows noticeable line broadening with increasing photon energy, which can be ascribed to the photon energy resolution. The lineshape is analyzed employing Voigt profiles, a combination of Lorentzian and Gaussian functions. The Lorentzian component represents the core hole lifetime, while the Gaussian component accounts for various factors, including the instrumental energy resolution for both photons and electrons. For simplicity in the fitting procedure, the phonon contribution is also assumed to produce Gaussian broadening.

$$\sigma = \sqrt{\sigma_{beamline}^2 + \sigma_{spect}^2 + \quad \sigma_{phonon}^2} \text{with FWHM} = 2\sqrt{2\ln 2} \bullet \sigma \qquad (2)$$

The energy resolution of the spectrometer is determined by the pass energy – slit combination, corresponding to a σ_{spect} value of 200 meV. The photon energy resolution of the beamline is determined by the monochromator spectral bandwidth and the photon source characteristics, which vary with photon energy (see Table 1).

In regard to the intrinsic hole lifetime broadening contribution, our simplified approach assigns this to the Lorentzian component of the Voigt profile. While this is not uniquely determined in our fits, we can estimate a value by observing the best agreement between the fitted curve and the experimental data, as indicated by an R factor analysis of the fits. This fits are executed employing using literature values for the experimentally determined lifetime broadening of Si 2p (65 meV), C 1s (70 meV), and 800 meV for Si 2s [17,18].

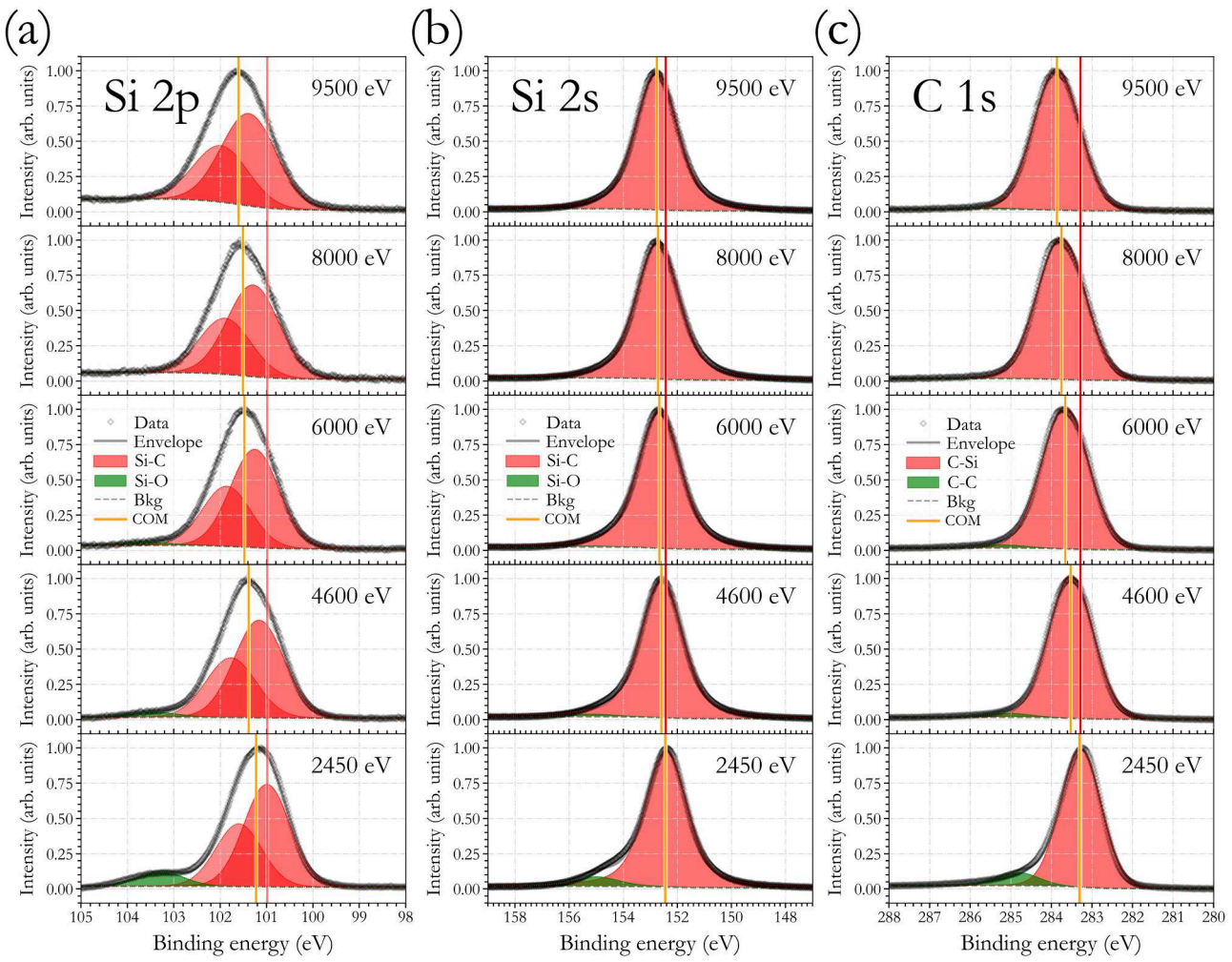

Fig. 2. HAXPES spectra of the Si 2p (a), Si 2s (b), and C 1s (c), core levels of 4H-SiC, measured at 5 different photon energies from 2.45 keV to 9.5 keV at room temperature. The thin red line marks the position of the main fit component at the lowest excitation energy (2450 eV), while the orange lines indicate the centroid of the unresolved photoemission line center. The green component in the SiC spectra is associated with a surface feature, which disappears at the highest excitation energies.

A closer examination of the SiC spectra in Fig. 2 reveals that, with an increase in photon energy, not only does the linewidth broaden, but the entire profile undergoes a change. In contrast, Si does not display comparable changes (see Fig. 1). The Au core level reference spectra from the Au overlayer on both samples show no shift or change in width under these conditions, however, the width of these lines is substantially larger [19]. The optimal modeling for the SiC lines requires incorporating an additional high-binding-energy satellite with the main core level lines. The best fit is obtained for a satellite positioned at 575 meV higher in binding energy for all lines, slightly less than the intrinsic spin-orbit splitting of the Si 2p lines. However, the inclusion of this satellite in the model is beyond the scope of the present study and further investigations are planned. Instead, the centroid of the line is indicated by the orange vertical line in Fig. 2 and the dashed orange line

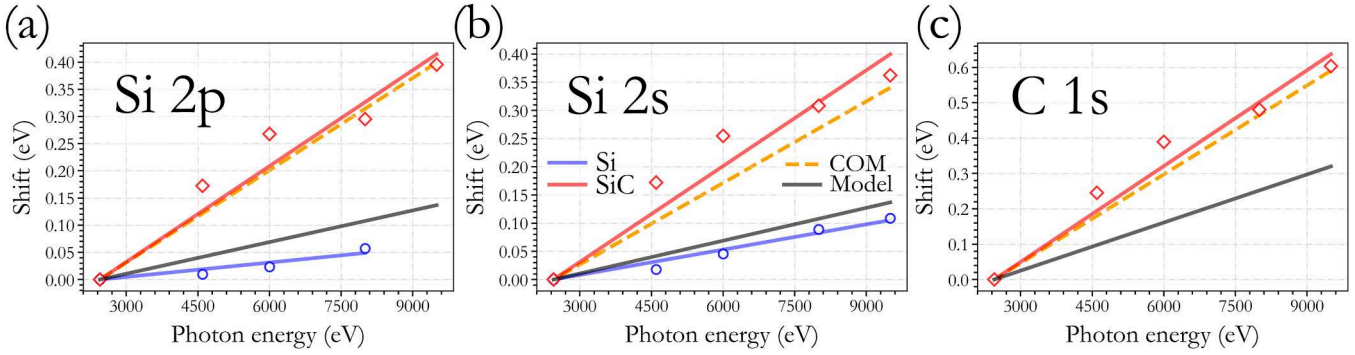

Fig. 3. Evaluated shifts of the Si 2p (a), Si 2s (b), and C 1s (c) core levels of n-type Si(100) (blue circles) and 4H-SiC (red diamonds). The values are given relative to the measured binding energy at the lowest excitation energy of 2.45 keV. The red (SiC) and blue (Si) solid lines represent linear fits to the evaluated recoil shifts. The orange dashed line shows the position of the centroid of the photoemission peak. The values for the free atom model (Eq. (1)) are shown by a black line.

in Fig. 3.

Turning our attention back to the recoil shift: for Si, the evaluation is straightforward, but for SiC it depends on assumptions about the lineshape composition. If we consider only the centroids of the peaks, the analysis presented above shows that with an increase in excitation energy from 2.45 keV to 9.5 keV the center of mass shift by 399 meV for the Si 2p, 340 meV for the Si 2s, and 590 meV for the C 1s level. These values are evidently larger than the predictions made by the simple atomic model (see Eq. (1)).

Even when assuming a complex line structure the shifts observed for the SiC core levels remain significantly larger than those predicted by the atomic model. The dashed orange line in Fig. 3 shows the shift of the center of mass of the peak. The shift values are referenced to the binding energy measured at the lowest photon energy of 2.45 keV. This approach reveals the same pattern as in the initial approach presented above: for SiC, all core levels exhibit a recoil shift exceeding the atomic model prediction, whereas for Si, the observed shifts fall below the line showing the free atom model. To the best of our knowledge, 4H-SiC remains the only reported case where the apparent recoil shift is larger than predicted by the atomic model.

What we observe here is a superposition of two effects. First, there is the photoelectron recoil, which manifests as a shift of the photoemission lines to apparently higher binding energies. Second, the excitation of phonon modes, which increases with the kinetic energy of the photoelectron. Together, these effects lead to a change in lineshape and an additional shift of the line centroid. The analogy to Mössbauer spectroscopy has been noted in the literature [4–10], even though there remains the difference due to the fact the Mössbauer spectroscopy concerns nuclear transitions and the photons are emitted by the nuclei while we here deal with electronic transitions of electrons which are (tighly) bound to the nucleus by Coulomb forces. High-resolution spectra of molecules exhibit this exact behavior [1]. The resulting lineshape change deviates from the Franck-Condon behavior, where the vibrational profile of the photoelectron is calculated based on the neutral state and the core-hole excited state, without explicitly accounting for the photoelectron kinetic energy.

Before further examining our results, let's first consider recoil processes within a classical model of photoemission from diatomic molecules (AB), as presented by E. Kukk et al. [1].

In the laboratory framework, momentum conservation requires that the electron momentum $p_e = \sqrt{2m_e E_{kin}}$ is balanced by the momentum of the center of mass motion of the entire molecule, resulting in a change in its translational energy, $E_{trans} = p_e^2/2(M_A + M_B)$. Assuming the core electron is localized on atom A, the recoil energy transferred to this atom in the photoemission process is given by $E_A = p_e^2/2M_A$.

Obviously, E_{trans} is smaller than E_A, indicating that only a part of the recoil energy is carried by the center of mass motion, with the residual energy being transferred into internal vibrational modes. Additionally, the smaller the mass of atom A, the more energy is diverted to internal degrees of freedom. This classical model was nicely confirmed by comparing C 1s emission from CH_4 and CF_4. In these molecules, the vibrational progression in the photoemission profile can be unambiguously identified, with CF_4 showing a much more pronounced vibrational profile than CH_4 due to the recoil effect [1].

How can we explain the difference between the results for SiC and Si? This can be attributed to the much stronger electron-phonon coupling in SiC compared to pure Si. This difference is evident from the Si 2p spectrum of SiC, where the spin-orbit splitting of the two core levels is obscured by vibrational coupling, as seen when comparing Figs. 1(a) and 2(a). A similar effect is observed when comparing the Si 2p core levels of Si with those of SiO_2. Compounds such as SiC and SiO_2 exhibit high-energy optical phonons, which are absent in crystalline Si. In fact, the Debye temperature of 4H-SiC (1200–1300 K) is nearly twice that of Si (640 K), and these phonons couple very effectively to the creation of a core-hole vacancy at all photon energies, significantly changing the photoemission lineshape. In this picture, the spectra of pure Si predominantly reflect the recoil effect, whereas in SiC, there is a substantial component due to the vibrational coupling that also varies with excitation energy.

4. Summary

This study examines recoil effects in photoemission for crystalline Si and 4H-SiC core levels under hard X-ray excitation, revealing significant changes in core level lineshape with photon energy. In SiC, recoil shifts for Si 2p, Si 2 s, and C 1s exceed single-atom model predictions, while the Si 2p and Si 2s shift in pure Si approximately aligns with these predictions. Our interpretation attributes this behavior to the excitation of high-energy optical phonons in SiC, driven by stronger electron-phonon coupling, which results in non-Franck-Condon behavior and modifies the vibrational envelope as photoelectron energy changes. These findings suggest that current models may require refinement, potentially through quantum mechanical calculations [20] that simultaneously incorporate recoil, Franck-Condon with anharmonicity, as well as effects beyond the Born-Oppenheimer approximation, to fully capture recoil behavior in polar materials like SiC. Furthermore, additional measurements at low temperatures are essential to fully disentangle temperature-dependent and phonon-mediated contributions to the recoil effects. Temperature dependent EXAFS could also provide some insights here.

Declaration of Competing Interest

The authors declare the following financial interests/personal relationships which may be considered as potential competing interests: Dmitrii Potorochin reports financial support and travel were provided by Federal Ministry of Education and Research Berlin Office. If there are other authors, they declare that they have no known competing financial interests or personal relationships that could have appeared to influence the work reported in this paper.

Acknowledgment

We acknowledge DESY (Hamburg, Germany), a member of the Helmholtz Association HGF, for the provision of experimental facilities. Parts of this research were carried out at PETRA III using beamline P22. Funding for the HAXPES instrument by the Federal Ministry of Education and Research (BMBF) under framework program ErUM is gratefully acknowledged. These experiments were supported within the research program 'structure of matter' of the Helmholtz Gemeinschaft (HGF). F. R. acknowledges financial support from DESY. This work was supported by the BMBF (Grant No. 05K22OF2 within ErUM-Pro).

Data availability

Data will be made available on request.

References

[1] E. Kukk, T.D. Thomas, K. Ueda, Recoil effects in molecular photoemission, J. Electron. Spectrosc. Relat. Phenom. 183 (2011) 53–58, https://doi.org/10.1016/j.elspec.2010.03.006.

[2] E. Kukk, D. Céolin, O. Travnikova, R. Püttner, M.N. Piancastelli, R. Guillemin, L. Journel, T. Marchenko, I. Ismail, J. Martins, J.-P. Rueff, M. Simon, Unified treatment of recoil and Doppler broadening in molecular high-energy photoemission, New J. Phys. 23 (2021) 063077, https://doi.org/10.1088/1367-2630/ac08b4.

[3] T. Hara, M. Yabashi, T. Tanaka, T. Bizen, S. Goto, X.M. Maréchal, T. Seike, K. Tamasaku, T. Ishikawa, H. Kitamura, The brightest x-ray source: a very long undulator at SPring-8, Rev. Sci. Instrum. 73 (2002) 1125–1128, https://doi.org/10.1063/1.1445866.

[4] C. Kalha, N.K. Fernando, P. Bhatt, F.O.L. Johansson, A. Lindblad, H. Rensmo, L. Z. Medina, R. Lindblad, S. Siol, L.P.H. Jeurgens, C. Cancellieri, K. Rossnagel, K. Medjanik, G. Schönhense, M. Simon, A.X. Gray, S. Nemšák, P. Lömker,

C. Schlueter, A. Regoutz, Hard x-ray photoelectron spectroscopy: a snapshot of the state-of-the-art in 2020, J. Phys.: Condens. Matter 33 (2021) 233001, https://doi.org/10.1088/1361-648X/abeacd.
[5] Y. Takata, Y. Kayanuma, M. Yabashi, K. Tamasaku, Y. Nishino, D. Miwa, Y. Harada, K. Horiba, S. Shin, S. Tanaka, E. Ikenaga, K. Kobayashi, Y. Senba, H. Ohashi, T. Ishikawa, Recoil effects of photoelectrons in a solid, Phys. Rev. B 75 (2007) 233404, https://doi.org/10.1103/PhysRevB.75.233404.
[6] Y. Takata, Y. Kayanuma, S. Oshima, S. Tanaka, M. Yabashi, K. Tamasaku, Y. Nishino, M. Matsunami, R. Eguchi, A. Chainani, M. Oura, T. Takeuchi, Y. Senba, H. Ohashi, S. Shin, T. Ishikawa, Recoil effect of photoelectrons in the fermi edge of simple metals, Phys. Rev. Lett. 101 (2008) 137601, https://doi.org/10.1103/PhysRevLett.101.137601.
[7] Y. Kayanuma, Recoil effects in X-ray photoelectron spectroscopy, in: J. Woicik (Ed.), Hard X-Ray Photoelectron Spectroscopy (HAXPES), Springer International Publishing, Cham, 2016, pp. 175–195, https://doi.org/10.1007/978-3-319-24043-5_8.
[8] A. Rattanachata, L.C. Nicolaï, H.P. Martins, G. Conti, M.J. Verstraete, M. Gehlmann, S. Ueda, K. Kobayashi, I. Vishik, C.M. Schneider, C.S. Fadley, A. X. Gray, J. Minár, S. Nemšák, Bulk electronic structure of lanthanum hexaboride ($\mathrm{La}{\mathrm{B}}_{6}$) by hard x-ray angle-resolved photoelectron spectroscopy, Phys. Rev. Mater. 5 (2021) 055002, https://doi.org/10.1103/PhysRevMaterials.5.055002.
[9] S. Suga, S. Itoda, A. Sekiyama, H. Fujiwara, S. Komori, S. Imada, M. Yabashi, K. Tamasaku, A. Higashiya, T. Ishikawa, M. Shang, T. Fujikawa, Recoil effects for valence and core photoelectrons in ${\mathrm{V}}_{3}$ Si, Phys. Rev. B 86 (2012) 035146, https://doi.org/10.1103/PhysRevB.86.035146.
[10] S. Suga, A. Sekiyama, H. Fujiwara, Y. Nakatsu, T. Miyamachi, S. Imada, P. Baltzer, S. Niitaka, H. Takagi, K. Yoshimura, M. Yabashi, K. Tamasaku, A. Higashiya, T. Ishikawa, Do all nuclei recoil on photoemission in compounds? New J. Phys. 11 (2009) 073025 https://doi.org/10.1088/1367-2630/11/7/073025.
[11] C. Schlueter, A. Gloskovskii, K. Ederer, I. Schostak, S. Piec, I. Sarkar, Yu Matveyev, P. Lömker, M. Sing, R. Claessen, C. Wiemann, C.M. Schneider, K. Medjanik, G. Schönhense, P. Amann, A. Nilsson, W. Drube, The new dedicated HAXPES beamline P22 at PETRAIII, AIP Conf. Proc. 2054 (2019) 040010, https://doi.org/10.1063/1.5084611.
[12] M. Newville, T. Stensitzki, D.B. Allen, A. Ingargiola, LMFIT: Non-Linear Least-Square Minimization and Curve-Fitting for Python, 2014. https://doi.org/10.5281/zenodo.11813.
[13] J.D. Hunter, Matplotlib: a 2D graphics environment, Comput. Sci. Eng. 9 (2007) 90–95, https://doi.org/10.1109/MCSE.2007.55.
[14] D.A. Shirley, High-resolution x-ray photoemission spectrum of the valence bands of gold, Phys. Rev. B 5 (1972) 4709–4714, https://doi.org/10.1103/PhysRevB.5.4709.
[15] M.T. Anthony, M.P. Seah, XPS: Energy calibration of electron spectrometers. 1—an absolute, traceable energy calibration and the provision of atomic reference line energies, Surf. Interface Anal. 6 (1984) 95–106, https://doi.org/10.1002/sia.740060302.
[16] N. Sieber, Th Seyller, L. Ley, D. James, J.D. Riley, R.C.G. Leckey, M. Polcik, Synchrotron x-ray photoelectron spectroscopy study of hydrogen-terminated $6H \ensuremath{-}\mathrm{SiC}{0001}$ surfaces, Phys. Rev. B 67 (2003) 205304, https://doi.org/10.1103/PhysRevB.67.205304.
[17] R. Püttner, T. Marchenko, R. Guillemin, L. Journel, G. Goldsztejn, D. Céolin, O. Takahashi, K. Ueda, A.F. Lago, M.N. Piancastelli, M. Simon, Si 1s−1, 2s−1 and 2p−1 lifetime broadening of SiX4 (X = F, Cl, Br, CH3) molecules: SiF4 anomalous behaviour reassessed, Phys. Chem. Chem. Phys. 21 (2019) 8827–8836, https://doi.org/10.1039/C8CP07369D.
[18] C. Nicolas, C. Miron, Lifetime broadening of core-excited and -ionized states, J. Electron. Spectrosc. Relat. Phenom. 185 (2012) 267–272, https://doi.org/10.1016/j.elspec.2012.05.008.
[19] M. Patanen, S. Aksela, S. Urpelainen, T. Kantia, S. Heinäsmäki, H. Aksela, Free atom 4f photoelectron spectra of Au, Pb, and Bi, J. Electron Spectrosc. Relat. Phenom. 183 (2011) 59–63, https://doi.org/10.1016/j.elspec.2010.01.008.
[20] T. Fujikawa, K. Niki, Phonon effects in high-energy photoemission spectra, J. Electron Spectrosc. Relat. Phenom. 280 (2025) 147525, https://doi.org/10.1016/j.elspec.2025.147525.